A FULL-WAVE ANALYSIS OF MICROSTRIP RESONATORS

Tatsuo Itoh
Department of Electrical Engineering
University of Illinois at Urbana-Champaign
Urbana, Illinois 61801

Abstract

An accurate and efficient method was developed for computing the resonant frequencies of microstrip resonators. The numerical data were compared with other theoretical and experimental results. The agreement of the numerical results with experimental data was extremely good.

Introduction

The microstrip and the disk resonators are useful integrated circuit components at microwave- and millimeter-wave frequencies. The analysis of such structures, however, has been undertaken under various approximations.[1,2] Since the design formulas so obtained are not very reliable, the designers of such circuit components are often forced to use cut-and-try methods to obtain desired resonant frequencies.

In this paper, a new method, based on the rigorous full-wave theory, will be reported for analyzing a rectangular microstrip resonator. The derivation of the characteristic equation for resonant frequency is carried out using Galerkin's method applied in the spectral domain as opposed to the conventional space domain analysis. The resonant frequencies are obtained by numerically solving the characteristic equation.

Method of Analysis

The microstrip resonator to be analyzed is shown in Fig. 1. A rectangular strip of width 2w and length 2ℓ is placed on the substrate which is, in turn, placed in a shield case. It is assumed that the thickness of the strip is negligible and that all the media are lossless. The shielding case and the substrate are assumed to extend to $z = \pm\infty$.

In the present structure, the fields, which are the superposition of TE (to z) and TM (to z) fields, can be expressed in terms of two types of scalar potentials $\phi(x,y,z)$ for TM and $\psi(x,y,z)$ for TE fields. Instead of solving the boundary value problems associated with the structure in the space domain, the analytical process will be carried out in the spectral or Fourier transform domain.[3] To this end let us define the Fourier transform of potential ϕ_i via

$$\tilde{\phi}_i(n,y,\beta) = \int_{-\infty}^{\infty} dz \int_{-a}^{a} dx\, \phi_i(x,y,z)\, e^{j\hat{k}_n x}\, e^{j\beta z} \tag{1}$$

and a similar equation for $\psi_i(x,y,z)$, where $i = 1, 2$ designates the substrate or the air region, and $\hat{k}_n = (n - 1/2)\pi/a$ for E_z even - H_z odd (in x) modes and $\hat{k}_n = n\pi/a$ for E_z odd - H_z even (in x) modes.

Imposing the boundary and continuity conditions at $y = 0, d$ and $d + h$ in the spectral domain, one obtains after some mathematical manipulations:

$$\tilde{G}_{11}(n,\beta,k_0)\tilde{J}_x(n,\beta) + \tilde{G}_{12}(n,\beta,k_0)\tilde{J}_z(n,\beta) = \tilde{E}_z(n,\beta) \tag{2a}$$

$$\tilde{G}_{21}(n,\beta,k_0)\tilde{J}_x(n,\beta) + \tilde{G}_{22}(n,\beta,k_0)\tilde{J}_z(n,\beta) = \tilde{E}_x(n,\beta) \tag{2b}$$

where

$$\tilde{G}_{11} = \tilde{G}_{22} = \hat{k}_n\beta(\gamma_2 \tanh \gamma_2 h + \mu_r\gamma_1 \tanh \gamma_1 d)/\det$$

$$\tilde{G}_{12} = \left[\left(\varepsilon_r\mu_r k_0^2 - \beta^2\right)\gamma_2 \tanh \gamma_2 h + \mu_r\left(k_0^2 - \beta^2\right)\gamma_1 \tanh \gamma_1 d\right]/\det$$

$$\tilde{G}_{21} = \left[\left(\varepsilon_r\mu_r k_0^2 - \hat{k}_n^2\right)\gamma_2 \tanh \gamma_2 h + \mu_r\left(k_0^2 - \hat{k}_n^2\right)\gamma_1 \tanh \gamma_1 d\right]/\det$$

$$\det = (\gamma_1 \tanh \gamma_1 d + \varepsilon_r\gamma_2 \tanh \gamma_2 h) \cdot (\gamma_1 \coth \gamma_1 d + \mu_r\gamma_2 \coth \gamma_2 h)$$

$$\gamma_1^2 = \hat{k}_n^2 + \beta^2 - \varepsilon_r\mu_r k_0^2, \quad \gamma_2^2 = \hat{k}_n^2 + \beta^2 - k_0^2, \quad k_0 = \text{free-space wavenumber} \tag{3}$$

and $\tilde{J}_x$ and $\tilde{J}_z$ are the transforms of induced strip current components J_x and J_z. $\tilde{E}_z$ and $\tilde{E}_x$ are proportional to the transforms of electric fields at $y = d$. Equations (2) are algebraic equations as opposed to the coupled integral equations appearing in the conventional space domain analysis.

Galerkin's method is then applied to Equation (2). $\tilde{J}_x$ and $\tilde{J}_z$ are first expressed in terms of basis functions $\tilde{J}_{xm}$ and $\tilde{J}_{zm}$ with unknown weight coefficients c_m and d_m. Substituting these expressions for $\tilde{J}_x$ and $\tilde{J}_z$ in Equation (2) and taking inner products of the resulting equations with $\tilde{J}_{xi}$ and $\tilde{J}_{zi}$, one obtains

$$\sum_{m=1}^{M} K_{im}^{(1,1)} c_m + \sum_{m=1}^{N} K_{im}^{(1,2)} d_m = 0, \quad i = 1, 2, \ldots, N \tag{4a}$$

$$\sum_{m=1}^{M} K_{im}^{(2,1)} c_m + \sum_{m=1}^{N} K_{im}^{(2,2)} d_m = 0 ,$$
$$i = 1, 2, \ldots, M \qquad (4b)$$

where

$$K_{im}^{(1,1)}(k_0) = \sum_{n=1}^{\infty} \int_0^{\infty} \tilde{J}_{zi}(n,\beta)\tilde{G}_{11}(n,\beta,k_0)\tilde{J}_{xm}(n,\beta)\, d\beta \qquad (5a)$$

$$K_{im}^{(1,2)}(k_0) = \sum_{n=1}^{\infty} \int_0^{\infty} \tilde{J}_{zi}(n,\beta)\tilde{G}_{12}(n,\beta,k_0)\tilde{J}_{zm}(n,\beta)\, d\beta \qquad (5b)$$

$$K_{im}^{(2,1)}(k_0) = \sum_{n=1}^{\infty} \int_0^{\infty} \tilde{J}_{xi}(n,\beta)\tilde{G}_{21}(n,\beta,k_0)\tilde{J}_{xm}(n,\beta)\, d\beta \qquad (5c)$$

$$K_{im}^{(2,2)}(k_0) = \sum_{n=1}^{\infty} \int_0^{\infty} \tilde{J}_{xi}(n,\beta)\tilde{G}_{22}(n,\beta,k_0)\tilde{J}_{zm}(n,\beta)\, d\beta . \qquad (5d)$$

Although Equation (2) contains four unknowns $\tilde{J}_x$, $\tilde{J}_z$, $\tilde{E}_x$ and $\tilde{E}_z$, note that the two latter unknowns have been eliminated in the derivation of Equation (4) via the application of Parseval's relation, because the inverse transforms of $\tilde{J}_{xm}$ and $\tilde{E}_x$ are nonzero only in the complementary regions in the xz plane at $y = d$ and because the same argument holds for J_{zm} and $\tilde{E}_z$.

The resonant frequency is obtained from the value of k_0 that makes the determinant of the coefficient matrix of Equation (4) zero. The numerical computation has been carried out for the dominant mode by letting $M = N = 1$ and choosing $\tilde{J}_{z1}$ and $\tilde{J}_{x1}$ to be the transforms of $J_{z1} = J_1(x)J_2(z)$ and $J_{x1} = J_3(x)J_4(z)$. The forms of J_1 to J_4 are plotted in Fig. 2. The infinite summations of infinite integrals can be evaluated efficiently since the integrands decrease as $(\hat{k}_n w)^{-3}$ and $(\beta \ell)^{-3}$.

The solution in the present method can be systematically improved by increasing the number of basis functions M and N and solving a larger matrix. The numerical efficiency is superior to many conventional space domain analyses since in the present method the algebraic equations rather than integral equations are solved.

Results and Discussion

The numerical computation based on the present theory has been carried out at the University of Illinois using a CDC G-20 computer which is several times slower than the IBM 360/75. Typical computation time was about 200 seconds per structure. An example of the results is plotted in Fig. 3 and compared with other theoretical and experimental data. Other theoretical results are based on the open-ended quasi-TEM and parallel-plate transmission line models. The latter is of width 2w and thickness d, has magnetic side walls, and is filled with medium of ε_r. In both of these approximation models, the resonant frequency was computed from the length $2(\ell + \Delta\ell)$ where $\Delta\ell = 0.3d$ is the hypothetical extension which accounts for the end effects.[4]

The experiments have been conducted at the Bell Laboratories using the 0.254 mm thick strip. The loaded Q of the resonant circuit was around 1500. As seen from Fig. 3, the agreement between the experimental data and the numerical results by the present method is extremely good. Table 1 shows that the agreement is even better if the loaded Q is increased.

Conclusions

A new efficient method based on the rigorous full-wave analysis has been developed for computing the resonant frequency of microstrip resonators. Numerical results agree extremely well with experimental data.

References

1. T. Itoh and R. Mittra, "Analysis of a microstrip disk resonator," Archiv für Elektronik und Übertragungstechnik, vol. 27, no. 11, pp. 456-458, November 1973.

2. J. Wolff and N. Knoppik, "Rectangular and circular microstrip disc-capacitors and -resonators," European Microwave Conference, B.4.1., Brussels, Belgium, September 1973.

3. T. Itoh and R. Mittra, "Spectral domain approach for calculating the dispersion characteristics of microstrip lines," IEEE Trans. Microwave Theory and Techniques, vol. MTT-21, no. 7, pp. 496-499, July 1973.

4. T. Itoh, R. Mittra and R. D. Ward, "A method for computing edge capacitance of finite and semi-infinite microstrip lines," IEEE Trans. Microwave Theory and Techniques, vol. MTT-20, no. 12, pp. 847-849, December 1972.

Acknowledgement

The author thanks Dr. W. W. Snell, Jr., of Bell Laboratories for the experimental data furnished. He also acknowledges the encouragement of Dr. M. V. Schneider of Bell Laboratories and Professor R. Mittra of the University of Illinois at Urbana-Champaign. This work was supported in part by the National Science Foundation, Grant No. NSF GK 36854 and in part by the U. S. Army, Grant No. DA-ARO-D-31-124-71-G77.

TABLE 1. RESONANT FREQUENCY VS. LOADED Q
(2ℓ = 10 cm resonator)

Loaded Q	Resonant Frequency (MHz)
37	708.0
106	730.6
466	742.3
688	743.0
1509	746.0
1735	746.4
2334	747.0
10000	753.0*
Present theory	752.4

* Extrapolated value.

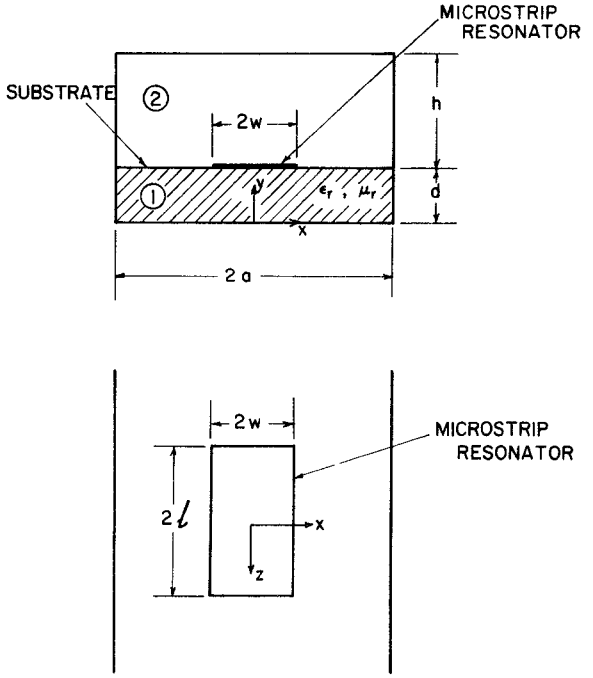

Fig. 1. End view and top view of microstrip resonator.

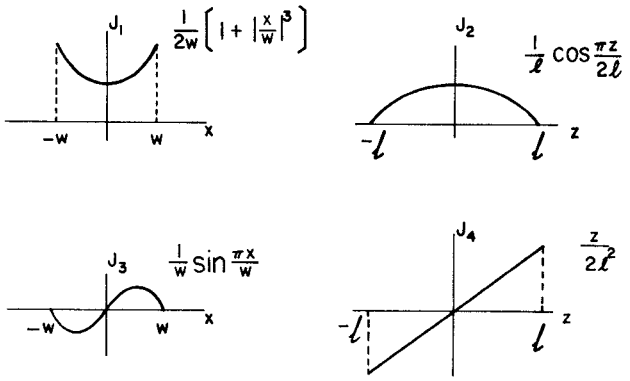

Fig. 2. Forms of current components used for the resonance calculation of dominant mode.

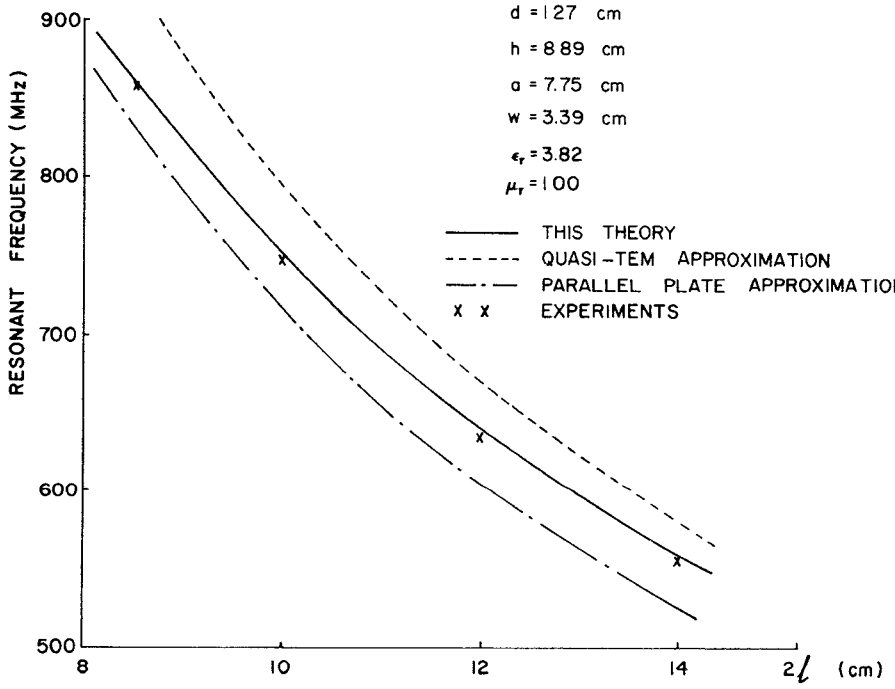

Fig. 3. Resonant frequency vs. the length of the resonator.